and all images were made at airmasses less than 1.2 with Gemini facility guiding and tip-tilt engaged. To improve the signal-to-noise ratio, the images displayed in Fig. 1 have been smoothed with gaussians of FWHM of 0.223, 0.223, 0.267, 0.356 and 0.445 arcsec at 8.7, 11.7, 12.3, 18.3 and 24.6 μm, respectively.

The probability that the SW 52 AU clump is a chance superposition of an unrelated background object is negligibly small ($<4 \times 10^{-5}$), as determined elsewhere[28] for a source of comparable brightness. Regarding the clumps apparent in the 24.6-μm image, we estimate the contrast of the brightest clump at SW 60 AU with the adjacent inner minimum to be approximately three times the noise, but the centroid of that clump is separated from the minimum (SW 52 AU) by less than the 24.6-μm resolution of 14 AU (Table 1). Thus, we make no firm judgement about the reality of the 24.6-μm clumps, ignoring for now the detailed 24.6-μm structure. We note that, if ultimately confirmed, it could provide significant additional insight into disk processes.

Dust mass and models

To characterize the NE disk emission, we considered a single population of dust grains with the commonly used approximation that the emission efficiency Q_ν is proportional to frequency. Other forms for Q_ν basically raise or lower the temperature and optical depth distributions, but our purpose, which is to contrast the dust properties in the NE and SW wings, is well served by our simple assumption. The assumed value for the stellar luminosity is $8.7L_\odot$, where $L_\odot$ is the luminosity of the Sun. The model disk extends out to 150 AU and is composed of 11 annuli that are 10 AU wide in the 0–110 AU region and one annulus that is 40 AU wide in the 110–150-AU region. We ignore results for the region within 20 AU of the star because of the contribution of the silicate feature and uncertainties in the PSF. Each annulus is assumed to be uniform in temperature and density. The modelling computes the distributions of temperature and face-on optical depth for the annuli that give rise to the brightness distributions observed at 11.7 and 18.3 μm. The models incorporate an inclination of the whole disk to the line of sight and opening angles as free parameters for each annulus. Optical depths and temperatures of the annuli were used to determine the flux in the appropriate wavebands emitted by the portion of the disk in a narrow radial range. The model is three-dimensional, with flux spread evenly in both latitude (in the range allowed by the disk opening angle) and longitude. The disk observations were simulated with the flux from the model being integrated along the line of sight of each pixel. The point-like stellar flux was then included at the centre. The image was then convolved with the PSF observed at the appropriate wavelength and additional smoothing added at the same level applied for the displayed images. The modelling procedure started with initial values for the annuli, then the parameters for each annulus were improved in turn by considering how varying them affected the resulting image. This procedure worked from the outermost to the innermost annulus and was repeated until the parameters converged. Uncertainties in the derived parameters were determined from the pixel-to-pixel deviation in the observation. A detailed description of the modelling for β Pic will be presented elsewhere by M.C.W. and co-workers.

Received 14 September; accepted 2 December 2004; doi:10.1038/nature03255.

1. Crifo, F., Vidal-Madjar, A., Lallement, R., Ferlet, R. & Gerbaldi, M. β Pictoris revisited by Hipparcos. Star properties. *Astron. Astrophys.* **320,** L29–L32 (1997).
2. Larwood, J. D. & Kalas, P. G. Close stellar encounters with planetesimal disks: the dynamics of asymmetry in the β Pictoris system. *Mon. Not. R. Astron. Soc.* **323,** 402–416 (2001).
3. Barrado y Navascués, D., Stauffer, J. R., Song, I. & Caillault, J.-P. The age of Beta Pictoris. *Astrophys. J.* **520,** L123–L126 (1999).
4. Zuckerman, B., Song, I., Bessell, M. S. & Webb, R. A. The β Pictoris moving group. *Astrophys. J.* **562,** L87–L90 (2001).
5. Heap, S. *et al.* Space telescope imaging spectrograph coronagraphic observations of β Pictoris. *Astrophys. J.* **539,** 435–444 (2000).
6. Mouillet, D., Larwood, J. D., Papaloizou, J. C. B. & Lagrange, A. M. A planet on an inclined orbit as an explanation of the warp in the β Pictoris disc. *Mon. Not. R. Astron. Soc.* **292,** 896–904 (1997).
7. Telesco, C. M., Becklin, E. E., Wolstencroft, R. D. & Decher, R. Resolution of the circumstellar disk of β Pictoris at 10 and 20 μm. *Nature* **335,** 51–53 (1988).
8. Backman, D. E., Gillett, F. C. & Witteborn, F. C. Infrared observations and thermal models of the β Pictoris dust disk. *Astrophys. J.* **385,** 670–679 (1992).
9. Lagage, P. O. & Pantin, E. Dust depletion in the inner disk of Beta Pictoris as a possible indicator of planets. *Nature* **369,** 628–630 (1994).
10. Pantin, E., Lagage, P. O. & Artymowicz, P. Mid-infrared images and models of the β Pictoris dust disk. *Astron. Astrophys.* **327,** 1123–1136 (1997).
11. Weinberger, A. J., Becklin, E. E. & Zuckerman, B. The first spatially resolved mid-infrared spectroscopy of β Pictoris. *Astrophys. J.* **584,** L33–L37 (2003).
12. Wahhaj, Z. *et al.* The inner rings of β Pictoris. *Astrophys. J.* **584,** L27–L31 (2003).
13. Okamoto, Y. K. *et al.* An extrasolar planetary system revealed by planetesimal belts in β Pictoris. *Nature* **431,** 660–662 (2004).
14. Li, A. & Greenberg, J. M. A comet dust model for the β Pictoris disk. *Astron. Astrophys.* **331,** 291–313 (1998).
15. Ozernoy, L. M., Gorkavyi, N. N., Mather, J. C. & Taidakova, T. A. Signatures of exosolar planets in dust disks. *Astrophys. J.* **537,** L147–L151 (2000).
16. Sicardy, B., Beaugé, C., Ferraz-Mello, S., Lazzaro, D. & Roques, F. Capture of grains into resonances through Poynting-Robertson drag. *Celest. Mech. Dyn. Astron.* **57,** 373–390 (1993).
17. Dermott, S. F., Jayaraman, S., Xu, Y. L., Gustafson, B. & Liou, J. C. A circumsolar ring of asteroidal dust in resonant lock with the Earth. *Nature* **369,** 719–723 (1994).
18. Wyatt, M. C. *et al.* How observations of circumstellar disk asymmetries can reveal hidden planets: pericenter glow and its application to the HR4796 disk. *Astrophys. J.* **527,** 918–944 (1999).
19. Wyatt, M. C. Resonant trapping of planetesimals by planet migration: debris disk clumps and Vega's similarity to the Solar System. *Astrophys. J.* **598,** 1321–1340 (2003).
20. Lagrange-Henri, A. M., Vidal-Madjar, A. & Ferlet, R. The β Pictoris circumstellar disk. VI. Evidence for material falling on to the star. *Astron. Astrophys.* **190,** 275–282 (1988).
21. Beust, H., Vidal-Madjar, A., Ferlat, R. & Lagrange-Henri, A. M. Cometary-like bodies in the protoplanetary disk around β Pictoris. *Astrophys. Space Sci.* **212,** 147–157 (1994).
22. Wyatt, M. C. & Dent, W. R. F. Collisional processes in extrasolar planetesimal discs—dust clumps in Fomalhaut's debris disc. *Mon. Not. R. Astron. Soc.* **334,** 589–607 (2002).
23. Brandeker, A., Liseau, R., Olofsson, G. & Fridlund, M. The spatial structure of the β Pictoris gas disk. *Astron. Astrophys.* **413,** 681–691 (2004).
24. Dominik, C. & Decin, G. Age dependence of the Vega phenomenon: theory. *Astrophys. J.* **598,** 626–635 (2003).
25. Hartmann, W. K. & Davis, D. R. Satellite-sized planetesimals and lunar origin. *Icarus* **24,** 504–515 (1975).
26. Dermott, S. F., Kehoe, T. J. J., Durda, D. D., Grogan, K. & Nesvorný, D. in *Asteroids, Comets, and Meteors 2002* (ed. Warmbein, B.) ESA SP-500, 319–322 (Publications Division, Noordwijk, 2002).
27. Kenyon, S. J. & Bromley, B. C. Detecting the dusty debris of terrestrial planet formation. *Astrophys. J.* **602,** L133–L136 (2004).
28. Van Paradijs, J., Telesco, C. M., Kouveliotou, C. & Fishman, G. J. 10 micron detection of the hard x-ray transient GRO J0422+32: free-free emission from an x-ray-driven accretion disk wind? *Astrophys. J.* **429,** L19–L23 (1994).

Acknowledgements We dedicate this paper to the memory of our colleague F. Gillett, infrared astronomy pioneer and co-discoverer of circumstellar debris disks. We thank K. Hanna, J. Julian and R. Piña for contributions to the success of T-ReCS; F. Varosi for assistance with data reduction; the Gemini Observatory staff in Chile, particularly M.-C. Hainaut-Rouelle, for technical assistance; and D. Simons of Gemini Observatory for support. This paper is based on observations (programme number GS-2003B-14) obtained at the Gemini Observatory, which is operated by the Association of Universities for Research in Astronomy, Inc., under a cooperative agreement with the NSF on behalf of the Gemini partnership: the National Science Foundation (United States), the Particle Physics and Astronomy Research Council (United Kingdom), the National Research Council (Canada), CONICYT (Chile), the Australian Research Council (Australia), CNPq (Brazil) and CONICET (Argentina). This research was funded in part by an NSF grant to C.M.T.

Competing interests statement The authors declare that they have no competing financial interests.

Correspondence and requests for materials should be addressed to C.M.T. (telesco@astro.ufl.edu).

Revised rates for the stellar triple-α process from measurement of ^{12}C nuclear resonances

Hans O. U. Fynbo[1], Christian Aa. Diget[1], Uffe C. Bergmann[2], Maria J. G. Borge[3], Joakim Cederkäll[2], Peter Dendooven[4], Luis M. Fraile[2], Serge Franchoo[2], Valentin N. Fedosseev[2], Brian R. Fulton[5], Wenxue Huang[6], Jussi Huikari[6], Henrik B. Jeppesen[1], Ari S. Jokinen[6,7], Peter Jones[6], Björn Jonson[8], Ulli Köster[2], Karlheinz Langanke[1], Mikael Meister[8], Thomas Nilsson[2], Göran Nyman[8], Yolanda Prezado[3], Karsten Riisager[1], Sami Rinta-Antila[6], Olof Tengblad[3], Manuela Turrion[3], Youbao Wang[6], Leonid Weissman[2], Katarina Wilhelmsen[8], Juha Äystö[6,7] & The ISOLDE Collaboration[2]

[1]*Department of Physics and Astronomy, University of Aarhus, 8000 Århus C, Denmark*
[2]*CERN, CH-1211 Geneva 23, Switzerland*
[3]*Instituto Estructura de la Materia, CSIC, Serrano 113bis, E-28006, Madrid, Spain*
[4]*KVI, Zernikelaan, 9747 AA Groningen, The Netherlands*
[5]*Department of Physics, University of York, Heslington, YO10 5DD, UK*
[6]*Department of Physics, University of Jyväskylä, FIN-40351 Jyväskylä, Finland*
[7]*Helsinki Institute of Physics, FIN-00014 University of Helsinki, Finland*
[8]*Experimental Physics, Chalmers University of Technology and Göteborg University, S-41296 Göteborg, Sweden*

In the centres of stars where the temperature is high enough, three α-particles (helium nuclei) are able to combine to form ^{12}C because of a resonant reaction leading to a nuclear excited state[1]. (Stars with masses greater than ~0.5 times that of the Sun will at some point in their lives have a central temperature high enough for this reaction to proceed.) Although the reaction rate is of critical significance for determining elemental abundances in the

Universe[1], and for determining the size of the iron core of a star just before it goes supernova[2], it has hitherto been insufficiently determined[2]. Here we report a measurement of the inverse process, where a ^{12}C nucleus decays to three α-particles. We find a dominant resonance at an energy of ~11 MeV, but do not confirm the presence of a resonance at 9.1 MeV (ref. 3). We show that interference between two resonances has important effects on our measured spectrum. Using these data, we calculate the triple-α rate for temperatures from 10^7 K to 10^{10} K and find significant deviations from the standard rates[3]. Our rate below ~5×10^7 K is higher than the previous standard, implying that the critical amounts of carbon that catalysed hydrogen burning in the first stars are produced twice as fast as previously believed[4]. At temperatures above 10^9 K, our rate is much less, which modifies predicted nucleosynthesis in supernovae[5,6].

The most important resonance in ^{12}C for astrophysics is situated 7.65 MeV above the ground state, and has spin and parity 0^+ (ref. 7). Hoyle suggested this resonance in 1953 in order to reproduce the observed abundances of ^{12}C and ^{16}O, respectively the fourth and third most abundant nuclear species in the Universe[8]. This so-called Hoyle resonance was soon discovered experimentally[9], and its properties were established[10] on the basis of a measurement of α-particles emitted in the β-decay of ^{12}B. In 1956 it was predicted[11] to have the structure of a linear chain of three α-particles, and it was further conjectured that there had to be another resonance at 9–10 MeV with spin-parity 2^+. A resonance was found soon after[12] at 10.1 MeV with a very large width of 3 MeV, but its spin-parity could only be determined as 0^+ or 2^+. The past half-century has brought little clarification to this problem, but the 2^+ resonance (at 9.1 MeV with width 0.56 MeV) is still included in the current NACRE (Nuclear Astrophysics Compilation of Reaction Rates) compilation of astrophysical reaction rates[3], where it enhances the $3\alpha \rightarrow {}^{12}$C reaction rate by more than an order of magnitude for temperatures above 10^9 K.

We use the β-decay of the two isotopes ^{12}N and ^{12}B, produced using the ISOL method (see Methods), to access the interesting resonances in ^{12}C. As a decisive improvement over previous measurements, our detection system (see Methods) allows us to construct the excitation energy in ^{12}C in a model-independent way when at least two of the α-particles are detected in coincidence. If all three α-particles are detected, the ^{12}C energy is just the sum of their energies added to the 3α-threshold energy of 7.275 MeV; if only two particles are detected, the missing energy can be calculated from energy and momentum conservation. The contour plot of Fig. 1 allows the break-up pattern of the resonances to be immediately identified. The structure observed at 8–11 MeV excitation energy is the elusive 10-MeV resonance. It decays to the 3α final state in a two-step process via the unbound ground state of ^{8}Be: the diagonal to the right comes from the α-particle emitted from ^{12}C; the broad region to the left comes from the two α-particles from ^{8}Be (this is the time-reverse of the triple-α reaction in stars). The 12.71-MeV resonance can be seen to decay differently, as discussed in detail elsewhere[13].

The events in Fig. 1 that follow the diagonal must originate from 0^+ or 2^+ resonances in ^{12}C owing to angular momentum and parity conservation. We use these events to extract the excitation energy spectra in Fig. 2. Apart from lower detection thresholds in the ^{12}B experiment and the difference in Q_β energies (see Methods), which explains why the ^{12}N spectrum extends to higher energies, the agreement between the experimental data sets is very good and supports the correctness of the spectrum. An R-matrix fit (see Methods) using the currently believed best values[7] (energy 10.3(3) MeV and width 3.0(7) MeV) to describe the resonance (dashed-dotted curve, Fig. 2a) is consistent with the old data, but clearly does not describe our improved data. The choice of 0^+ or 2^+ for the spin gives the same quality of the fit to the old data. In contrast, only when we assume spin 0^+ for the 10-MeV resonance and include the 0^+ resonance at 7.65 MeV can we fit our data (Fig. 2b), owing to the inevitable interference effects caused by coherent population of two resonances with identical spin-parity[14]. The presence of a separate resonance at high energy in the ^{12}N data, already suggested in Fig. 1 by the continuation of the diagonal up to more than 14 MeV, becomes very clear in the spectra of Fig. 2. When including this high-energy region in the analysis, we have to introduce a new resonance to fit the data. A 0^+ assignment for this resonance will not fit our data owing to interference with the lower two 0^+ resonances, but when we assume a 2^+ resonance we get a good reproduction of the data (Fig. 2b). We determine the energy of the 10-MeV resonance to be 11.23(5) MeV with width 2.5(2) MeV, and the 2^+ contribution gives 13.9(3) MeV with width 0.7(3) MeV.

Our results are in qualitative agreement with recent ^{12}C(α,α′)^{12}C experiments[15,16], which observe a dominant 0^+ component in the 10-MeV region. However, our data clearly demonstrate the importance of including the appropriate interference between the two 0^+ resonances. The 2^+ resonance observed near 14 MeV in our data is

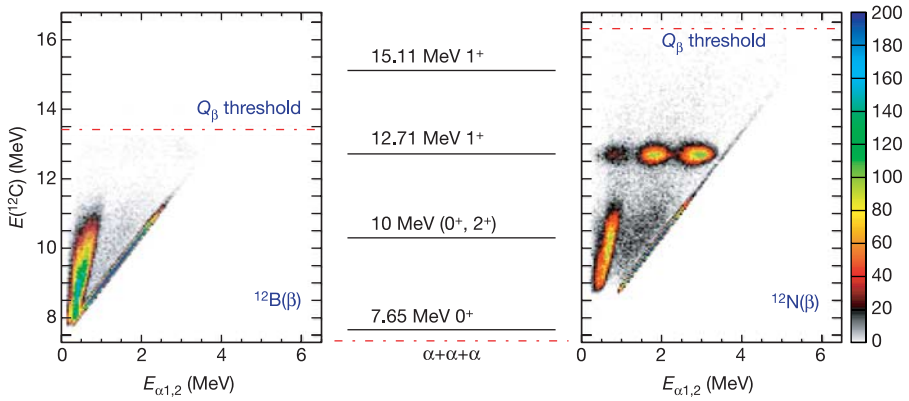

Figure 1 α-particles emitted from resonances in ^{12}C populated in the decays of ^{12}B and ^{12}N. The central panel shows the four resonances previously observed in these decays. The contour plots (colour levels given on vertical bar give the number of counts per pixel) show the excitation energy in ^{12}C, $E(^{12}C)$, plotted against the energy of individual α-particles, $E\alpha_{1,2}$; Q_β, energy released by nucleus in β-decay. Left panel, ^{12}B; right panel, ^{12}N. In our data, the 7.65-MeV resonance is below the detection threshold and therefore not observed, the broad 10-MeV resonance is identified in both decays, whereas the 12.71-MeV resonance is clearly seen in the ^{12}N data and weakly in the ^{12}B data. The 15.11-MeV resonance mainly decays by γ-emission and is therefore not observed.

consistent with earlier $^{12}C(e,e')^{12}C$ experiments[7], but is not observed in the recent $^{12}C(\alpha,\alpha')^{12}C$ experiments[15,16]. We have searched for a 2^+ resonance with the properties given in the NACRE compilation (position at 9.1 MeV, width 0.56 MeV). The ft-value (see Methods) for feeding such a resonance must be at least a factor of 50 larger than the one for the Hoyle resonance to fit our data. This seems unlikely, and the existence of this resonance is therefore doubtful.

We now turn to the implications of our findings for the synthesis of ^{12}C in the Universe: we estimate the influence on the triple-α reaction rate of the broad 0^+ resonance and its interference with the Hoyle resonance, and the effect of removing the assumed 2^+ state. For temperatures between 10^8 K and 10^9 K, the rate is fully dominated by the Hoyle resonance and may be determined by a simple expression depending exclusively on the properties of that resonance[1]. The calculation of the rate outside this temperature range is the subject of several specialized papers focusing on specific temperature regions, and is a subject of considerable complication. Details of the rate calculation are beyond the scope of this Letter; we use an expression that is general enough to be valid for temperatures from 10^7 K to 10^{10} K, and which includes the influence of the broad 0^+ resonance (C.D., H.F. and K.R., manuscript in preparation). By comparing our rate calculations (Fig. 3) with and without the presence of the broad 0^+ resonance, we conclude that this resonance does not introduce a significantly increased uncertainty to the rate despite its clear interference with the Hoyle resonance (Fig. 2). Considering that the rates vary more than 80 orders of magnitude over the illustrated temperature range, there is good general agreement between our rates and the NACRE rate. In the most important temperature range of 10^8 K to 10^9 K, our rate agrees with the rate calculated from the simple expression[1], whereas there is a systematic deviation from the NACRE rate that reaches 20% at 10^8 K, just beyond their quoted error band. For the lowest temperatures, and even more so for temperatures above 10^9 K, our rate deviates significantly from NACRE. The latter is due to their inclusion of an assumed 2^+ resonance at 9.1 MeV, an assumption that could not be confirmed in this work.

The triple-α reaction is crucial for various astrophysical scenarios. Its ratio with the rate of the subsequent $^{12}C(\alpha,\gamma)^{16}O$ reaction in the temperature range between 10^8 K and 10^9 K determines the carbon and oxygen abundances at the end of helium burning[17], with important consequences for both nucleosynthesis and late-stage stellar evolution[18]. The size of the iron core in the pre-supernova depends directly on this rate, and calls for better than 10% precision of the triple-α rate in the 10^8 K to 10^9 K temperature range for use in core-collapse supernovae simulations[2]. The carbon and oxygen production as function of the triple-α rate is investigated in ref. 19. The triple-α rate above 10^9 K is important for nucleosynthesis in the type II supernova shock front[5,6] where, owing to the high binding energy of ^{12}C, the triple-α process is the first reaction to fall out of equilibrium at relatively high temperatures of 3×10^9 K (ref. 20). The effect of our lower rate for these high temperatures is estimated as a reduction (by a factor of 2–3) of the mass fraction of ^{56}Ni, and hence a reduction of the mass fraction of heavy elements present in proton-rich supernova matter (C. Fröhlich, personal communication). These high temperatures are also relevant for X-ray bursts, which are explained as thermonuclear runaways in the hydrogen-rich envelope of an accreting neutron star in a binary system. One trigger reaction of the runaway is the triple-α reaction[21], which produces CNO nuclei that later serve as the material for the main energy production in the early stage of the burst[22]. A better precision of the triple-α rate is also needed to determine the ratio of ^{12}C to ^{16}O produced in the special conditions of helium

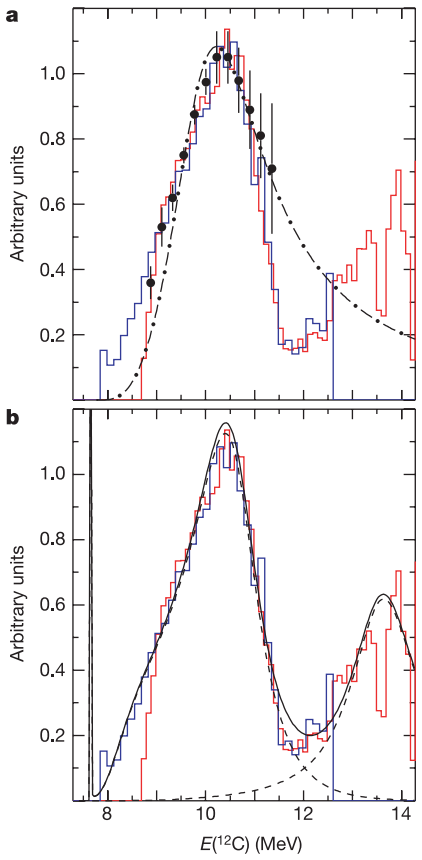

Figure 2 Excitation energy spectra in ^{12}C. The spectra are corrected for the different β-neutrino phase-space factors, and for detection efficiencies (arbitrary units on vertical axis). Data from $^{12}N/^{12}B$ decay are shown as the red/blue histograms. **a**, Comparison of our spectra with that from the last published measurement using β-decay[30] (filled circles; error bars, 1σ). The dashed-dotted curve shows the 10-MeV resonance using the literature values before the experiment reported here. **b**, Our fit (solid curve), where the 7.65-MeV 0^+ resonance, and a 2^+ resonance at high energy, are added (the individual components are shown with the dashed curves).

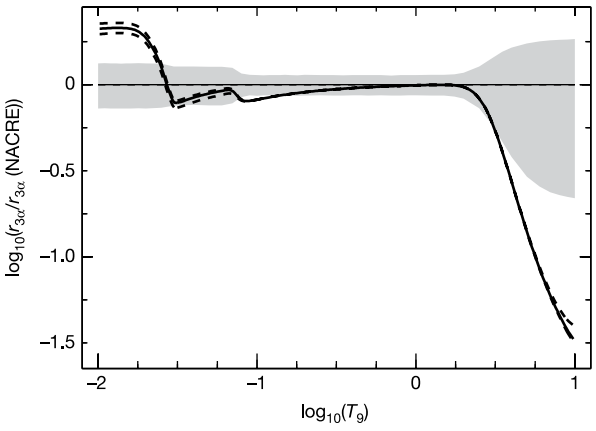

Figure 3 The triple-α reaction rate from this work, $r_{3\alpha}$, relative to the value from the current NACRE compilation[3], $r_{3\alpha}$(NACRE). T_9 is the temperature in 10^9 K. Solid line, our rate including only the Hoyle resonance; dashed lines, our rate including the broad 0^+ resonance and its interference with the Hoyle resonance; and grey band, estimated error band from NACRE[3] (the uncertainty in the position of their assumed 2^+ resonance is not included). We assume that the reduced γ-decay width of the broad 0^+ resonance is equal to that of the Hoyle resonance, and the dashed lines differ only in the sign of the interference term.

flashes during the asymptotic giant branch phase of stellar evolution (AGB stars); such stars have been identified as the site of the main component of s-process nucleosynthesis[23]. According to estimates given in refs 2 and 24, the consequence of our modified rate is up to a factor of 3 less carbon produced in AGB stars.

Finally, as the first stars in the Universe lacked the heavy elements catalysing hydrogen burning, the evolution of these stars is believed to be very sensitive to the triple-α reaction at temperatures below 10^8 K. For these primordial stars with masses similar to that of the Sun, a small amount of ^{12}C is produced by the triple-α process during the phase of central hydrogen burning. When the ^{12}C abundance reaches a critical level the CNO cycle is ignited[4]; this level may be reached in half the time with our higher rate at the lowest temperatures. This is important for the subsequent evolution of the star, and for how the ashes of the nuclear burning, the basis for the next generation of stars, are transported to the outer layers of the star and ejected into the interstellar medium. Stellar model calculations testing this effect using our triple-α rate are in progress (J. Christensen-Dalsgaard, personal communication). □

Methods

The ISOL method

The ^{12}N activity (half-life 11.0 ms) was produced at the IGISOL facility[25] of the Jyväskylä Accelerator Laboratory in Finland by using the ^{12}C(p,n)^{12}N reaction with a 40-MeV proton beam. The ^{12}B activity (half-life 20.20 ms) came from *in situ* decay of ^{12}Be (half-life 21.5 ms) produced by 1-GeV proton-induced spallation reactions on a thick Ta target at the ISOLDE facility[26], CERN. In both experiments, the produced nuclei were extracted, accelerated to 40 keV, mass separated and finally transferred to a detection area where they were stopped in a thin carbon collection foil. This is known as the isotope separation on-line (ISOL) method.

By studying the β-decays of both ^{12}B and ^{12}N we reduce sensitivity for systematic errors. These two nuclei release significantly different energies in their β-decays (known as the Q_β energy), which causes different excitation energies in ^{12}C to be populated with different weights owing to the strong energy dependence of the β-neutrino phase-space. The product of this phase-space factor and the partial half-life of a transition is the ft-value, which is inversely proportional to the nuclear matrix element.

Detection system

The detection system consisted of two double sided silicon strip detectors (DSSSDs) placed on either side of the collection foil. Owing to the presence of very low energy α-particles in these decays, attention to energy loss effects in the collection foil and detector dead-layers is crucial. In the ^{12}N experiment, standard DSSSDs were used and a special calibration and analysis procedure applied[27], whereas in the ^{12}B experiment a new DSSSD design with reduced dead-layers was used[28]. Significantly reduced energy detection thresholds were achieved in the ^{12}B experiment, as may be seen in Fig. 2 where the ^{12}B spectrum extends well below that from ^{12}N. The efficiency for detecting two or three α-particles is determined from Monte Carlo simulations separately for the two experiments.

R-matrix fits

These are commonly used in atomic, nuclear and particle physics to achieve a phenomenological understanding of data[14]. We apply a formalism developed specifically for β-decay[29]. The method is used in general to connect observed peak structures with parameter values of the states involved, in particular when interference effects or threshold effects are dominant. In such cases, the position of states does not always coincide with maxima of peaks in the observed spectra. The parameter values quoted here are the so-called observed R-matrix parameters, which are introduced to correct for this discrepancy. Here we use the same parameters for the Hoyle resonance as NACRE: resonance energy 0.3798 MeV, α-width 8.3 eV and γ-width 3.7 meV. The interference effect is seen in Fig. 2 as an enhancement of the low-energy region between the two resonances and a decrease on the high-energy side of the broad resonance. It causes the shift of the energy of the broad 0^+ resonance from the previous value near 10 MeV to 11.23(5) MeV even when using observed R-matrix parameters.

Received 7 September; accepted 24 November 2004; doi:10.1038/nature03219.

1. Wallerstein, G. *et al.* Synthesis of the elements in stars: 40 years of progress. *Rev. Mod. Phys.* **69,** 995–1084 (1997).
2. Austin, S. in *Proc. 8th Nuclei in the Cosmos Conf., Nucl. Phys. A* (in the press).
3. Angulo, C. *et al.* A compilation of charged-particle induced thermonuclear reaction rates. *Nucl. Phys. A* **656,** 3–183 (1999).
4. Siess, L., Livio, M. & Lattanzio, J. Structure, evolution, and nucleosynthesis of primordial stars. *Astrophys. J.* **570,** 329–343 (2002).
5. Fröhlich, C. *et al.* Composition of the innermost supernova ejecta. *Astrophys. J.* (submitted).
6. Pruet, J., Woosley, S. E., Buras, R., Janka, H.-T. & Hofmann, R. D. Nucleosynthesis in the hot convective bubble in core-collapse supernovae. *Astrophys. J.* (submitted).
7. Ajzenberg-Selove, F. Energy levels of light nuclei A=11–12. *Nucl. Phys. A* **506,** 1–158 (1990).
8. Hoyle, F., Dunbar, D. N. F., Wenzel, W. A. & Whaling, W. A state in ^{12}C predicted from astrophysical evidence. *Phys. Rev.* **92,** 1095 (1953).
9. Dunbar, D. N. F., Pixley, R. E., Wenzel, W. A. & Whaling, W. The 7.68 MeV state in ^{12}C. *Phys. Rev.* **92,** 649–650 (1953).
10. Cook, C. W., Fowler, W. A., Lauritsen, C. C. & Lauritsen, T. B^{12}, C^{12}, and the red giants. *Phys. Rev.* **107,** 508–515 (1957).
11. Morinaga, H. Interpretation of some of the excited states of 4n self-conjugate nuclei. *Phys. Rev.* **101,** 254–258 (1956).
12. Cook, C. W., Fowler, W. A., Lauritsen, C. C. & Lauritsen, T. High energy alpha particles from B^{12}. *Phys. Rev.* **111,** 567–571 (1958).
13. Fynbo, H. O. U. *et al.* Clarification of the three-body decay of ^{12}C(12.71 MeV). *Phys. Rev. Lett.* **91,** 082502 (2003).
14. Lane, A. M. & Thomas, R. G. R-matrix theory of nuclear reactions. *Rev. Mod. Phys.* **30,** 257–353 (1958).
15. John, B., Tokimoto, Y., Lui, Y.-W., Clark, H. L., Chen, X. & Youngblood, D. H. Isoscalar electric multipole strength in ^{12}C. *Phys. Rev. C* **68,** 014305 (2003).
16. Itoh, M. *et al.* Study of the cluster state at $E_x = 10.3$ MeV in ^{12}C. *Nucl. Phys. A* **738,** 268–272 (2004).
17. Fowler, W. A. Experimental and theoretical nuclear astrophysics: The quest for the origin of the elements. *Rev. Mod. Phys.* **56,** 149–179 (1984).
18. Weaver, T. A. & Woosley, S. E. Nucleosynthesis in massive stars and the ^{12}C(α,γ)^{16}O reaction rate. *Phys. Rep.* **227,** 65–96 (1993).
19. Schlattl, H., Heger, A., Oberhummer, H., Rauscher, T. & Csótó, A. Sensitivity of the C and O production on the 3α rate. *Astrophys. Space Sci.* **291,** 27–56 (2004).
20. Delano, M. D. & Cameron, A. G. W. Nucleosynthesis in neutron rich supernova ejecta. *Astrophys. Space Sci.* **10,** 203–226 (1971).
21. Schatz, H. *et al.* Rp-process nucleosynthesis at extreme temperature and density conditions. *Phys. Rep.* **294,** 167–263 (1998).
22. Woosley, S. E. *et al.* Models for Type I X-ray bursts with improved nuclear physics. *Astrophys. J. Supp.* **151,** 75–102 (2004).
23. Käppeler, F., Thielemann, F.-K. & Wiescher, M. Current quests in nuclear astrophysics and experimental approaches. *Annu. Rev. Part. Sci.* **48,** 175–251 (1998).
24. Herwig, F. & Austin, S. M. Nuclear reaction rates and carbon star formation. *Astrophys. J.* **613,** L73–L76 (2004).
25. Äystö, J. Development and applications of the IGISOL technique. *Nucl. Phys. A* **693,** 477–494 (2001).
26. Kugler, E. The ISOLDE facility. *Hyperfine Interact.* **129,** 23–42 (2000).
27. Bergmann, U. C., Fynbo, H. O. U. & Tengblad, O. Use of Si strip detectors for low-energy particles in compact geometry. *Nucl. Instrum. Methods A* **515,** 657–664 (2003).
28. Tengblad, O., Bergmann, U. C., Fraile, L. M., Fynbo, H. O. U. & Walsh, S. Novel thin window design for a large-area silicon strip detector. *Nucl. Instrum. Methods A* **525,** 458–464 (2004).
29. Barker, F. C. & Warburton, E. K. The beta-decay of ^{8}He. *Nucl. Phys. A* **487,** 269–278 (1988).
30. Schwalm, D. & Povh, B. Alpha particles following the β-decay of ^{12}B and ^{12}N. *Nucl. Phys.* **89,** 401–411 (1966).

Acknowledgements This research was supported by the Academy of Finland under the Finnish Centre of Excellence Programme, by the Spanish Agency CICYT, and by the European Union Fifth Framework Programme 'Improving Human Potential—Access to Research Infrastructure'. Discussions with J. Christensen-Dalsgaard and C. Fröhlich are acknowledged.

Competing interests statement The authors declare that they have no competing financial interests.

Correspondence and requests for materials should be addressed to H.F. (fynbo@phys.au.dk).

Systematic design of chemical oscillators using complexation and precipitation equilibria

Krisztina Kurin-Csörgei[1], Irving R. Epstein[2] & Miklós Orbán[1]

[1]*Department of Inorganic and Analytical Chemistry, L. Eötvös University, H-1518 Budapest 112, PO Box 32, Hungary*
[2]*Department of Chemistry and Volen Center for Complex Systems, MS 015, Brandeis University, Waltham, Massachusetts 02454-9110, USA*

Concentration oscillations are ubiquitous in living systems, where they involve a wide range of chemical species. In contrast, early *in vitro* chemical oscillators were all derived from two accidentally discovered reactions[1–3] based on oxyhalogen chemistry. Over the past 25 years, the use of a systematic design algorithm[4,5], in which a slow feedback reaction periodically drives a bistable system in a flow reactor between its two steady states, has increased the list of oscillating chemical reactions to dozens of systems. But these oscillating reactions are still con-